INTRODUCTION

CETP (cholesteryl ester transfer protein) is a key player in the metabolism of major plasma lipoproteins. CETP mediates the transfer of cholesteryl esters from HDL (high-density lipoprotein) to Apo (apolipoprotein) B-containing lipoproteins in exchange for triacylglycerols (triglycerides) [1]. CETP activities are known to be highly affected by genetic factors. For example, individuals with homozygous CETP deficiency have high HDL-C (HDL-cholesterol) levels and low LDL-C [LDL (low-density lipoprotein)-cholesterol] levels, and have no evidence of premature atherosclerosis [2]. Also, *CETP* gene polymorphisms, especially the *Taq*IB polymorphism identified in intron 1, is reported to be highly associated with plasma CETP concentrations and HDL-C levels. Moreover, recent meta-analyses revealed that this polymorphism is associated with the incidence of CAD (coronary artery disease) [3–7]. However, this polymorphism is unlikely to be functional by itself, instead representing a surrogate marker of functional variants of the *CETP* gene [8]. Indeed, previous studies have shown that the *CETP* promoter −629 A > C polymorphism has almost complete linkage disequilibrium with the *Taq*IB polymorphism [9,10], and that this polymorphism is associated with CAD [11]. On the other hand, we have reported [8] that the haplotype block consisting of −2668 G/A, −2505 C/A, −1337 C/T and the shortest (gaaa) repeat had a stronger association than *Taq*IB2 or −629 A/C with low plasma CETP concentrations and high HDL-C levels in healthy Japanese males. Moreover, functional interaction between −629 C/A, −971 G/A and −1337 C/T polymorphisms in the *CETP* gene is a major determinant of promoter activity and plasma CETP concentration in REGRESS (Regression Growth Evaluation Statin Study) [12].

In addition to CETP, HL (hepatic lipase) also plays a crucial role in the metabolism of plasma lipoproteins. HL is involved in the hydrolysis of triacylglycerol and phospholipids in IDL (intermediate-density lipoprotein) and large LDL particles to form smaller and denser LDL particles, and also plays a major role in promoting the conversion from HDL_2 into HDL_3 particles [13]. The effects of the *LIPC* genotype (the gene encoding HL) on atherosclerosis have been controversial [14], and may be dependent on LDL-receptor activity.

FH (familial hypercholesterolaemia) is an autosomal-dominant disorder characterized by primary hypercholesterolaemia with tendon xanthomas and premature CAD caused by mutations in the LDL receptor [15,16]. Mortality from CAD is reported to be several times higher in subjects with heterozygous FH than in the general population [15,16]. There are several reports that polymorphisms or mutations in the *CETP* gene influence the clinical characteristics of FH subjects [17,18]. Carmena-Ramon et al. [17] reported that in FH the *Taq*IB2 allele was associated with higher HDL-C and ApoAI levels. On the other hand, our previous study [18] showed that increased HDL-C levels caused by a heterozygous CETP deficiency was insufficient to prevent CAD in FH.

With this background, the present study investigated the effects of *CETP* promoter −1337 C > T and *LIPC* promoter −514 C > T polymorphisms on coronary atherosclerosis in Japanese patients with heterozygous FH.

METHODS

Study participants

We enrolled 206 consecutive Japanese patients with heterozygous FH (26–83 years old; 154 males) who attended our hospital. FH was diagnosed when one of the following two criteria was met: (i) primary hypercholesterolaemia [> 5.96 mmol/l (> 230 mg/dl) in any age group] in a patient with tendon xanthomas, or (ii) primary hypercholesterolaemia with a definitive diagnosis of FH in any first-degree relative [19]. All the females were postmenopausal, as defined by the absence of menstruation for > 6 months or having attained an age of ⩾ 60 years. Those with surgical menopause were excluded. For patients with MI (myocardial infarction), the age at the first event was recorded, whereas for patients with AP (angina pectoris), the age at which coronary angiography was performed was recorded. Inclusion criteria for this study were FH patients who were examined by coronary angiography because of chest symptoms and/or a positive exercise test before lipid-lowering therapy was initiated. Individuals who had thyroid disease, levels of triacylglycerol ⩾ 4.52 mmol/l (> 400 mg/dl) or who received lipid-lowering agents, corticosteroid or oestrogen hormone replacement therapy were excluded. All patients provided informed consent for participation in the present study, which was approved by the Ethical committee of Kanazawa University Graduate School of Medical Science.

Assessment of CAD

For the evaluation of CAD, we used CSI (coronary stenosis index) to quantify the severity of coronary atherosclerosis. The severity of stenotic changes was assessed by a score assigned to each of the 15 segments according to the classification of the American Heart Association Grading Committee. A normal coronary angiogram was graded as 0, stenosis of < 25 % was graded as 1, 25–50 % stenosis was graded as 2, 50–75 % stenosis was graded as 3, and > 75 % stenosis was graded as 4. CSI was defined as the sum of these scores in all 15 segments, producing a maximal value of 60 [15]. In the present study, MI was diagnosed in 56 subjects with

heterozygous FH (48 male), and AP was diagnosed in 53 subjects with heterozygous FH (all male). The mean CSI was 14.0 ± 11. The mean CSI in subjects who were diagnosed with MI and AP was 20, whereas the mean CSI in those subjects who were without clinical symptoms of CAD was 8. In our previous study [15], we observed that the age of coronary artery stenosis detectable by angiogram occurs after 17–25 years of age in male and female subjects with heterozygous FH. In the present study, 86 % of the subjects with MI and AP had a CSI > 14, whereas 80 % of subjects without clinical symptoms of CAD had a CSI < 14. Therefore we diagnosed CAD as being present when CSI was > 14.

Assessment of conventional risk factors

Data for BMI (body mass index), smoking history, alcohol drinking, blood pressure, diabetes status and lipid profile were collected. Hypertension was considered to be present if any antihypertensive treatment had been instituted, if systolic blood pressure was > 160 mmHg or diastolic blood pressure > 95 mmHg. Diabetes mellitus was diagnosed if fasting plasma glucose was ⩾ 6.70 mmol/l (> 120 mg/dl) or ⩾ 11.10 mmol/l (> 200 mg/dl) at 120 min after 75 g of oral glucose loading, or if HbA_{1c} (glycated haemoglobin) was ⩾ 6.5 %. For smoking status, we defined subjects who smoked ⩽ 10 cigarettes/day as non-smokers, past smokers as ex-smokers and current smokers.

Laboratory analysis

Blood samples were collected from subjects after 12 h of fasting before starting lipid-lowering agents. Total cholesterol, triacylglycerols and HDL-C levels were determined by standard enzymatic methods. LDL-C levels were calculated using the Friedewald formula [20]. Plasma CETP levels were determined by sandwich ELISA, as described previously [21].

Determination of *CETP* and *LIPC* promoter polymorphisms

Genomic DNA was isolated and purified from peripheral white blood cells. The *CETP* promoter −1337 C > T polymorphism and the *LIPC* promoter −514 C > T polymorphism (−480 in older reports) were analysed by PCR-RFLP (restriction-fragment-length polymorphism) methods, as described previously [8,22]. Accession numbers are as follows: *CETP*, gene ID 1071 [NCBI (National Center for Biotechnology Information) Entrez Gene database], nulceotide sequence NM_000078 (NCBI Entrez Nucleotide database) and −1337C/T SNP rs17231506 (NCBI SNP database); and *LIPC*, gene ID 3990 (NCBI Entrez Gene database), nucleotide sequence NM_000236 (NCBI Entrez Nucleotide database), −514 C/T SNP rs1800588 (NCBI SNP database) and −514 C/T USF binding site cctttgaca(c/t)gggggtgaag.

Table 1 Characteristics of subjects in this study

Values are means ± S.E.M. HDL-C* was adjusted by multiple linear regression analysis, including gender, alcohol intake, smoking and BMI.

Parameter	CAD	non-CAD	*P* value
Gender (male/female)	77/17	77/35	0.0303
Age (years)	52 ± 12	50 ± 12	0.3001
BMI (kg/m^2)	23.7 ± 3.0	23.9 ± 2.7	0.5000
Total cholesterol (nmol/l)	8.34 ± 1.74	8.37 ± 1.63	0.9131
Triacylglycerol (nmol/l)	1.64 ± 0.69	1.65 ± 0.80	0.8618
HDL-C (nmol/l)	1.04 ± 0.28	1.09 ± 0.34	0.2052
HDL-C* (mmol/l)	1.17 ± 0.28	1.22 ± 0.31	0.3888
LDL-C (nmol/l)	6.55 ± 1.79	6.53 ± 1.66	0.8658
ApoAI (g/l)	1.01 ± 0.25	1.08 ± 0.24	0.1222
ApoB (g/l)	1.77 ± 0.53	1.78 ± 0.44	0.9052
ApoE (g/l)	0.06 ± 0.03	0.06 ± 0.02	0.7330
Hypertension (*n*)	32 (34.0 %)	20 (17.9 %)	0.0070
Diabetes mellitus (*n*)	34 (36.2 %)	22 (19.6 %)	0.0079
Smokers (*n*)	54 (57.4 %)	63 (56.2 %)	0.8629
Alcohol drinkers (*n*)	36 (38.3 %)	44 (39.3 %)	0.8848
CSI	23.7 ± 7.4	5.8 ± 4.3	< 0.0001

Statistical analyses

All values are expressed as means ± S.D. unless otherwise noted. The allele frequency was estimated by gene counting. One-way ANOVA was performed, followed by multiple comparisons using Fisher's protected least significant difference. Serum HDL-C was adjusted by multiple linear regression analysis. The prevalence of patients with hypertension, diabetes mellitus, current and past smoking, and alcohol drinking were compared between different groups using a χ^2 test. A multiple logistic regression analysis was used to predict CAD from the genotype of polymorphism, with conventional risk factors as covariates. A probability value of $P < 0.05$ was considered to be significant. All tests were performed with StatView software (version 5.0; SAS Institute).

RESULTS

Characteristics of study subjects

The clinical and biochemical characteristics of the study population either with CAD or without CAD (non-CAD) are summarized in Table 1. A total of 94 the subjects with heterozygotes FH were suffering from CAD. There were significantly more males and subjects with hypertension and diabetes mellitus in the CAD group compared with the non-CAD group.

Association between −1337 C > T polymorphism and CSI

The frequency of the *CETP* promoter −1337 T allele was 0.20 in both males and females; lower than in Caucasians [12]. A few subjects in the present study had

Table 2 ***CETP*** **− 1337 C > T polymorphism and plasma CETP levels**

P value was determined using χ^2 test.

	CETP genotype				
	− 1337 CC		− 1337 CT + TT		
	n	CETP (μg/ml)	*n*	CETP (μg/ml)	*P* value
All	31	3.1 ± 1.1	13	2.6 ± 0.6	0.1364
Male	17	2.6 ± 0.6	8	2.4 ± 0.6	0.3139
Female	14	3.6 ± 1.3	5	3.0 ± 0.5	0.2831

the *CETP* promoter − 1337 TT genotype (11 males and two females), and the T allele was less frequent in subjects with a CSI ⩾ 14. The distribution of the *CETP* promoter − 1337 CC genotype differed significantly between those with a CSI ⩾ 14 and those with a CSI < 14 ($P = 0.0426$, as determined by a χ^2 test).

CETP promoter polymorphism and CETP concentrations

We compared plasma CETP concentrations between the − 1337 CC and − 1337 CT + TT genotypes in a subset of 44 subjects (25 males; Table 2). The CETP concentration tended to be lower in the presence of the T allele ($P = 0.14$).

CETP promoter polymorphism, lipid profile and development of CAD

The characteristics of subjects according to *CETP* promoter polymorphism are summarized in Table 3. As there were only two females with the TT genotype, we analysed men and women combined. HDL-C levels were not significantly higher in TT genotype, and the CSI tended to be lower in patients carrying the T allele ($P = 0.19$).

Effects of *CETP* and *LIPC* promoter polymorphisms on lipid profile and CSI

The frequency of the *LIPC* promoter − 514 T allele was 0.53 in males and 0.50 in females, which is similar to the frequencies previously reported in Japanese subjects, but higher than those in Caucasians [22,23]. To investigate the effects of *CETP* and *LIPC* promoter polymorphisms on lipid profile, we compared four subgroups stratified by high *CETP* genotype CC compared with low CETP CT + TT, and high *LIPC* genotype CC compared with low *LIPC* genotype CT + TT. Figure 1 shows that the HDL-C level was significantly higher in − 514 CC/− 1337 CT + TT than in − 514 CC/− 1337 CC [1.22 ± 0.36 mmol/l (47 ± 14 mg/dl) compared with 0.98 ± 0.30 mmol/l (38 ± 10 mg/dl) respectively; $P < 0.02$], and it was significantly higher in − 514 CC/− 1337 CT + TT than in − 514 CT + TT/− 1337 CC or in both CT + TT ($P < 0.05$). LDL-C levels did not differ significantly between the four groups. CSI was significantly lower in − 514 CC/− 1337 CT + TT than in − 514 CC/− 1337 CC (9.6 compared with 17.2 respectively; $P = 0.02$), suggesting an interaction between *CETP* and *LIPC* genotype on CSI.

Table 3 **Characteristics of the subjects according to** ***CETP*** **genotype status**

Values are means ± S.E.M. HDL-C* was adjusted by multiple linear regression analysis, including gender, alcohol intake, smoking and BMI.

	CETP genotype		
	CC	CT	TT
n	127	66	13
Total cholesterol (nmol/l)	8.50 ± 1.71	8.18 ± 1.66	7.87 ± 1.27
Triacylglycerol (nmol/l)	1.62 ± 0.72	1.73 ± 0.82	1.48 ± 0.57
HDL-C (nmol/l)	1.04 ± 0.28	1.09 ± 0.37	1.17 ± 0.37
HDL-C* (mmol/l)	1.19 ± 0.28	1.22 ± 0.37	1.23 ± 0.37
LDL-C (nmol/l)	6.71 ± 1.81	6.29 ± 1.61	6.03 ± 1.24
ApoAI (g/l)	1.02 ± 0.25	1.09 ± 0.25	1.08 ± 0.21
ApoB(g/l)	1.81 ± 0.50	1.76 ± 0.47	1.66 ± 0.36
ApoE(g/l)	0.07 ± 0.03	0.07 ± 0.03	0.05 ± 0.02
Age (years)	50 ± 11	53 ± 13	48 ± 11
BMI (kg/m^2)	23.7 ± 2.7	24.3 ± 3.2	22.8 ± 2.5
Smokers (%)	69 (54.3)	38 (57.6)	10 (76.9)
Hypertension (%)	30 (23.6)	18 (27.3)	4 (30.8)
Diabetes mellitus (%)	35 (27.6)	19 (28.8)	2 (15.4)
CSI	15.0 ± 10.7	12.4 ± 10.6	11.6 ± 9.6

Multiple logistic regression analysis

A multiple logistic regression analysis was performed to determine the association of CAD and *CETP* promoter polymorphism and other conventional risk factors. Gender, hypertension, diabetes mellitus and *CETP* − 1337 CC genotype exhibited significantly higher odds ratios; however, age, smoking, HDL-C and triacylglycerol levels, and the presence of *LIPC* − 514 C > T were not significant variates (Table 4).

DISCUSSION

The present study investigated the effects of *CETP* and *LIPC* promoter polymorphisms on serum lipid profiles and risk of coronary atherosclerosis in subjects with heterozygous FH. None of the other coronary risk factors differed significantly between *CETP* genotypes; however, multiple logistic regression analysis revealed that coronary atherosclerosis was associated with the *CETP* − 1337 CC genotype. An interaction between the *CETP* and *LIPC* genotypes for plasma HDL-C and CAD has also been shown.

To our knowledge, this is the first study on the effects of the *CETP* promoter − 1337 C > T polymorphism

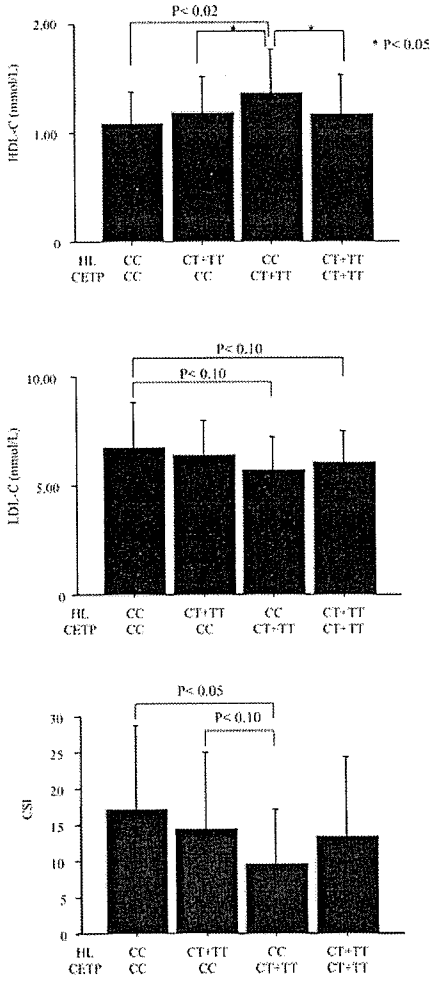

Figure 1 Effects of *CETP* and *LIPC* promoter polymorphisms on LDL-C, HDL-C and CSI

Subjects: −514 CC/−1337 CT+TT ($n=29$); −514 CT+TT/−1337 CC ($n=98$); −514 CC /−1337 CT+TT ($n=17$); −514 CT+TT/−1337 CT+TT ($n=62$). The HDL-C level was significantly higher in −514 CC/−1337 CT+TT than in −514 CC/−1337 CC (1.22 ± 0.36 compared with 0.98 ± 0.03 mmol/l; $P<0.02$), and it was significantly higher in −514 CC/−1337 CT+TT than in −514 CT+TT/−1337 CC or CT+TT ($P<0.05$). The LDL-C levels did not differ significantly between the four groups. CSI was significantly lower in −514 CC/−1337 CT+TT subjects than in −514 CC/−1337 CC subjects (9.6 compared with 17.2; $P=0.02$).

in coronary atherosclerosis and, therefore, the first to suggest that the *CETP* promoter −1337 C>T polymorphism is associated with the severity of coronary atherosclerosis in heterozygous FH. In a previous study [8], this polymorphism was associated with low plasma CETP concentrations and high HDL-C levels more strongly than with the *Taq*IB2 allele in elderly Japanese males and, recently, this polymorphism has been reported to be a major determinant of promoter activity and plasma CETP concentration in REGRESS [12]. Therefore we

Table 4 Multivariate adjusted relative prevalence odds ratio of coronary atherosclerosis by multiple logistic regression analysis

For sex, male = 1 and female = 0; for hypertension, yes = 1 and no = 0; for diabetes mellitus, yes = 1 and no = 0; for *CETP* −1337 C>T polymorphism, CC = 1 and T+ = 0; for *LIPC* −514 C>T polymorphism, CC = 2, CT = 1 and TT = 0.

Variate	Odds ratio	*P* value
Age	1.021 (0.993–1.050)	0.1431
Sex	4.283 (1.788–10.259)	0.0011
Hypertension	2.628 (1.252–5.519)	0.0107
Diabetes mellitus	2.136 (1.081–4.218)	0.0289
Smoking	0.992 (0.969–1.015)	0.3261
CETP −1337 C>T polymorphism	2.022 (1.090–3.754)	0.0256
LIPC −514 C>T polymorphism	0.856 (0.562–1.305)	0.4698

investigated this −1337 site rather than the well-known *Taq*IB polymorphism. As subjects with FH have a high risk of premature CAD, we determined the existence of early stage coronary atherosclerotic changes by using CSI. Our present data suggest that the association of the *CETP* genotype with cardiovascular risk is independent of serum HDL-C levels. As indicated in Table 3, there was no significant difference in HDL-C/adjusted HDL-C levels between *CETP* genotypes. The *CETP Taq*IB2 allele was associated with HDL-C, especially HDL_2-C, in Japanese subjects [24] and, therefore, if we had assessed HDL_2-C, this might have revealed a significant difference between the genotypes.

There are conflicting reports as to whether CETP is pro- or anti-atherogenic. Humans with homozygous CETP deficiency have markedly high HDL-C levels and decreased LDL-C levels, with no clear evidence of premature atherosclerosis [2]. A *CETP* gene mutation (D442G) was shown to be associated with increased LDL particle size [25], suggesting that CETP is pro-atherogenic. In contrast, Hirano et al. [26] have reported that the prevalence of CETP deficiency was lower in individuals older than 80 years of age residing in a district of northern Japan, suggesting that CETP deficiency is not association with longevity, and the same investigators have shown that reduced CETP activity in conjunction with reduced HL activity is associated with an increased risk of CAD [27]. On the other hand, Moriyama et al. [28] found in a cross-sectional analysis that HDL-C elevation (⩾ 80 mg/dl) was protective against coronary heart disease, regardless of *CETP* genotype, in 19044 male and 29487 female Japanese subjects. In addition, a recent prospective study in the Honolulu Heart Program has shown the protective effects of heterozygous CETP deficiency against CAD, although the effect was not statistically significant [29].

At lower CETP concentrations, LDL-receptor activity is up-regulated, causing a reduction in serum LDL levels and leading to atheroprotection. Lowering CETP activity may be beneficial in an affluent environment, where high-fat and cholesterol-rich diets increase plasma LDL-C levels and down-regulate hepatic LDL-receptors, such as in FH. We presume that individuals with FH have higher CETP activity or concentration than normolipidaemic controls [30,31], which would be less pro-atherogenetic when they carry the *CETP* promoter −1337 T allele. De Grooth et al. [32] reported a significant positive correlation between carotid intima-media thickness and CETP levels in FH, suggesting that plasma CETP would be pro-atherogenic in FH. There are also some reports on the *CETP Taq*IB polymorphism and impaired glucose tolerance [33], suggesting that CETP could be pro-atherogenic independently of lipid metabolism. In the present study, however, there was no significant difference between *CETP* promoter −1337 C > T polymorphism and serum glucose levels (5.99 ± 1.94 mmol/l in −1337 CC compared with 5.72 ± 1.33 mmol/l in −1337 CT + TT; $P = 0.20$), and no difference in diabetes prevalence (results not shown).

In addition to CETP, HL also plays a crucial role in the metabolism of plasma lipoproteins, but the effects of CETP and HL activity on lipid profile and CAD are unclear [14,34]. The present study found no association between the *LIPC* promoter −514 C > T polymorphism and CAD and HDL-C levels; however, CSI with the *CETP* −1337 T allele and *LIPC* −514 CC was lowest in the subgroup. In another study from our laboratory (M. Takata and A. Inazu, unpublished work), HL activity was significant higher in −514 CC than CT + TT (0.282 ± 0.011 compared 0.231 ± 0.005 mmol/l respectively, $P < 0.001$) in hyperlipidaemic patients ($n = 325$, of which 183 were male). In human studies, HL activity tends to be elevated in the presence of smoking [35], insulin resistance in Type II diabetes mellitus [36], in females with omental fat mass [37] and males in general. These reports suggest that HL is pro-atherogenic. On the other hand, it has been reported that HL activity is lower in patients with CAD than in those without CAD [38]. Another group found that HL activity did not differ between subjects with and without CAD in REGRESS [39]. In an environment of low HL activity, IDL increases and it may be pro-atherogenic [40]. HL also promotes the formation of small and dense atherogenic LDL particles [13]. Lowering HL activity in hypertriglyceridaemia may decrease the pro-atherogenic risk due to an improved lipid profile, notably an increased LDL size [14]. In conditions where LDL-receptor activity is low, as in FH, HL activity appears to be inversely associated with CAD in subjects with low CETP concentrations (Figure 1), suggesting that the flux of cholesterol through the system of HDL-C transport may be more important in preventing atherosclerosis.

The main limitations of the present study were the relatively small sample size and the absence of data on HDL subclass and LDL particle size.

In conclusion, the *CETP* promoter −1337 C > T polymorphism is associated with the progression of coronary atherosclerosis in Japanese patients with FH, independent of HDL-C and triacylglycerol levels. We believe that this genetic variant of the *CETP* gene promoter could be an important determinant of coronary atherosclerosis in FH, and genotype differences between promoter variants and missense mutations need to be clarified in future investigations.

ACKNOWLEDGMENTS

We express special thanks to the lipidologists and cardiologists at the Second Department of Internal Medicine, Kanazawa University, and also to Sachio Yamamoto, Mihoko Mizuno and Mayumi Yoshida for their technical assistance. This work was supported by the Scientific Research Grant from the Ministry of Education, Science and Culture of Japan (no. 10770568 and 0907010).

REFERENCES

1 Tall, A. R. (1993) Plasma cholesteryl ester transfer protein. J. Lipid Res. **34**, 1255–1274
2 Inazu, A., Brown, M. L., Hesler, C. B. et al. (1990) Increased high-density lipoprotein levels caused by a common cholesteryl-ester transfer protein gene mutation. N. Engl. J. Med. **323**, 1234–1238
3 Kuivenhoven, J. A., Jukema, J. W., Zwinderman, A. H. et al. (1998) The role of a common variant of the cholesteryl ester transfer protein gene in the progression of coronary atherosclerosis. The Regression Growth Evaluation Statin Study Group. N. Engl. J. Med. **338**, 86–93
4 Kuivenhoven, J. A., de Knijff, P., Boer, J. M. et al. (1997) Heterogeneity at the CETP gene locus. Influence on plasma CETP concentrations and HDL cholesterol levels. Arterioscler., Thromb., Vasc. Biol. **17**, 560–568
5 Ordovas, J. M., Cupples, L. A., Corella, D. et al. (2000) Association of cholesteryl ester transfer protein-TaqIB polymorphism with variations in lipoprotein subclasses and coronary heart disease risk: the Framingham study. Arterioscler., Thromb., Vasc. Biol. **20**, 1323–1329
6 Carlquist, J. F., Muhlestein, J. B., Horne, B. D. et al. (2003) The cholesteryl ester transfer protein Taq1B gene polymorphism predicts clinical benefit of statin therapy in patients with significant coronary artery disease. Am. Heart J. **146**, 1007–1014
7 Boekholdt, S. M., Sacks, F. M., Jukema, J. W. et al. (2005) Cholesteryl ester transfer protein TaqIB variant, high-density lipoprotein cholesterol levels, cardiovascular risk, and efficacy of pravastatin treatment: individual patient meta-analysis of 13 677 subjects. Circulation **111**, 278–287
8 Lu, H., Inazu, A., Moriyama, Y. et al. (2003) Haplotype analyses of cholesteryl ester transfer protein gene promoter: a clue to an unsolved mystery of TaqIB polymorphism. J. Mol. Med. **81**, 246–255
9 Dachet, C., Poirier, O., Cambien, F., Chapman, J. and Rouis, M. (2000) New functional promoter polymorphism, CETP/−629, in cholesteryl ester transfer protein (CETP) gene related to CETP mass and high density lipoprotein cholesterol levels: role of Sp1/Sp3 in transcriptional regulation. Arterioscler., Thromb., Vasc. Biol. **20**, 507–515

10 Klerkx, A. H., Tanck, M. W., Kastelein, J. J. et al. (2003) Haplotype analysis of the CETP gene: not TaqIB, but the closely linked -629C→A polymorphism and a novel promoter variant are independently associated with CETP concentration. Hum. Mol. Genet. **12**, 111–123
11 Blankenberg, S., Rupprecht, H. J., Bickel, C. et al. (2003) Common genetic variation of the cholesteryl ester transfer protein gene strongly predicts future cardiovascular death in patients with coronary artery disease. J. Am. Coll. Cardiol. **41**, 1983–1989
12 Frisdal, E., Klerkx, A. H., Le Goff, W. et al. (2005) Functional interaction between −629C/A, −971G/A and −1337C/T polymorphisms in the CETP gene is a major determinant of promoter activity and plasma CETP concentration in the REGRESS Study. Hum. Mol. Genet. **14**, 2607–2618
13 Kuusi, T., Saarinen, P. and Nikkila, E. A. (1980) Evidence for the role of hepatic endothelial lipase in the metabolism of plasma high density lipoprotein 2 in man. Atherosclerosis **36**, 589–593
14 Jansen, H., Verhoeven, A. J. and Sijbrands, E. J. (2002) Hepatic lipase: a pro- or anti-atherogenic protein? J. Lipid Res. **43**, 1352–1362
15 Mabuchi, H., Koizumi, J., Shimizu, M. and Takeda, R. (1989) Development of coronary heart disease in familial hypercholesterolemia. Circulation **79**, 225–232
16 Goldstein, J. L., Hobbs, H. H., Brown, M. S. et al. (2001) Familial hypercholesterolemia. In The Metabolic and Molecular Bases of Inherited Disease, vol. 2, 8th ed. (Scriver, C. R., Beaudet, A. L., Sly, W. S. et al., eds.), pp. 2863–2913, McGraw-Hill, New York
17 Carmena-Ramon, R., Ascaso, J. F., Real, J. T., Najera, G., Ordovas, J. M. and Carmena, R. (2001) Association between the TaqIB polymorphism in the cholesteryl ester transfer protein gene locus and plasma lipoprotein levels in familial hypercholesterolemia. Metab., Clin. Exp. **50**, 651–656
18 Haraki, T., Inazu, A., Yagi, K., Kajinami, K., Koizumi, J. and Mabuchi, H. (1997) Clinical characteristics of double heterozygotes with familial hypercholesterolemia and cholesteryl ester transfer protein deficiency. Atherosclerosis **132**, 229–236
19 Mabuchi, H., Higashikata, T., Nohara, A. et al. (2005) Cutoff point separating affected and unaffected familial hypercholesterolemic patients validated by LDL-receptor gene mutants. J. Atheroscler. Thromb. **12**, 35–40
20 Friedewald, W. T., Levy, R. I. and Fredrickson, D. S. (1972) Estimation of the concentration of low-density lipoprotein cholesterol in plasma, without use of the preparative ultracentrifuge. Clin. Chem. **18**, 499–502
21 Kiyohara, T., Kiriyama, R., Zamma, S. et al. (1998) Enzyme immunoassay for cholesteryl ester transfer protein in human serum. Clin. Chim. Acta **271**, 109–118
22 Inazu, A., Nishimura, Y., Terada, Y. and Mabuchi, H. (2001) Effects of hepatic lipase gene promoter nucleotide variations on serum HDL cholesterol concentration in the general Japanese population. J. Hum. Genet. **46**, 172–177
23 Carr, M. C., Brunzell, J. D. and Deeb, S. S. (2004) Ethnic differences in hepatic lipase and HDL in Japanese, black, and white Americans: role of central obesity and LIPC polymorphisms. J. Lipid Res. **45**, 466–473
24 Ikewaki, K., Mabuchi, H., Teramoto, T. et al. (2003) Japan CETP Study Group. Association of cholesteryl ester transfer protein activity and TaqIB polymorphism with lipoprotein variations in Japanese subjects. Metab., Clin. Exp. **52**, 1564–1570
25 Wang, J., Qiang, H., Chen, D., Zhang, C. and Zhuang, Y. (2002) CETP gene mutation (D442G) increases low-density lipoprotein particle size in patients with coronary heart disease. Clin. Chim. Acta **322**, 85–90
26 Hirano, K., Yamashita, S., Nakajima, N. et al. (1997) Genetic cholesteryl ester transfer protein deficiency is extremely frequent in the Omagari area of Japan. Marked hyperalphalipoproteinemia caused by CETP gene mutation is not associated with longevity. Arterioscler., Thromb., Vasc. Biol. **17**, 1053–1059
27 Hirano, K., Yamashita, S., Kuga, Y. et al. (1995) Atherosclerotic disease in marked hyperalphalipoproteinemia. Combined reduction of cholesteryl ester transfer protein and hepatic triglyceride lipase. Arterioscler., Thromb., Vasc. Biol. **15**, 1849–1856
28 Moriyama, Y., Okamura, T., Inazu, A. et al. (1998) A low prevalence of coronary heart disease among subjects with increased high-density lipoprotein cholesterol levels, including those with plasma cholesteryl ester transfer protein deficiency. Prev. Med. **27**, 659–667
29 Curb, J. D., Abbott, R. D., Rodriguez, B. L. et al. (2004) A prospective study of HDL-C and cholesteryl ester transfer protein gene mutations and the risk of coronary heart disease in the elderly. J. Lipid Res. **45**, 948–953
30 Inazu, A., Koizumi, J., Mabuchi, H., Kajinami, K. and Takeda, R. (1992) Enhanced cholesteryl ester transfer protein activities and abnormalities of high density lipoproteins in familial hypercholesterolemia. Horm. Metab. Res. **24**, 284–288
31 Hogue, J. C., Lamarche, B., Gaudet, D. et al. (2004) Relationship between cholesteryl ester transfer protein and LDL heterogeneity in familial hypercholesterolemia. J. Lipid Res. **45**, 1077–1083
32 de Grooth, G. J., Smilde, T. J., Van Wissen, S. et al. (2004) The relationship between cholesteryl ester transfer protein levels and risk factor profile in patients with familial hypercholesterolemia. Atherosclerosis **173**, 261–267
33 Weitgasser, R., Galvan, G., Malaimare, L. et al. (2004) Cholesteryl ester transfer protein TaqIB polymorphism and its relation to parameters of the insulin resistance syndrome in an Austrian cohort. Biomed. Pharmacother. **58**, 619–627
34 de Grooth, G. J., Klerkx, A. H., Stroes, E. S., Stalenhoef, A. F., Kastelein, J. J. and Kuivenhoven, J. A. (2004) A review of CETP and its relation to atherosclerosis. J. Lipid Res. **45**, 1967–1974
35 Kong, C., Nimmo, L., Elatrozy, T. et al. (2001) Smoking is associated with increased hepatic lipase activity, insulin resistance, dyslipidaemia and early atherosclerosis in Type 2 diabetes. Atherosclerosis **156**, 373–378
36 Baynes, C., Henderson, A. D., Anyaoku, V. et al. (1991) The role of insulin insensitivity and hepatic lipase in the dyslipidaemia of type 2 diabetes. Diabetic Med. **8**, 560–566
37 Carr, M. C., Hokanson, J. E., Zambon, A. et al. (2001) The contribution of intraabdominal fat to gender differences in hepatic lipase activity and low/high density lipoprotein heterogeneity. J. Clin. Endocrinol. Metab. **86**, 2831–2837
38 Dugi, K. A., Brandauer, K., Schmidt, N. et al. (2001) Low hepatic lipase activity is a novel risk factor for coronary artery disease. Circulation. **104**, 3057–3062
39 Jansen, H., Verhoeven, A. J., Weeks, L. et al. (1997) Common C-to-T substitution at position -480 of the hepatic lipase promoter associated with a lowered lipase activity in coronary artery disease patients. Arterioscler., Thromb., Vasc. Biol. **17**, 2837–2842
40 Hodis, H. N., Mack, W. J., Dunn, M. et al. (1997) Intermediate-density lipoproteins and progression of carotid arterial wall intima-media thickness. Circulation **95**, 2022–2022

Received 20 April 2006/21 June 2006; accepted 6 July 2006
Published as Immediate Publication 6 July 2006, doi:10.1042/CS20060088

Cardiac Resurrection After Bone-Marrow-Derived Mononuclear Cell Transplantation During Left Ventricular Assist Device Support

Satoshi Gojo, MD, PhD, Shunei Kyo, MD, PhD,
Shigeyuki Nishimura, MD, PhD,
Nobuyuki Komiyama, MD, PhD,
Nobutaka Kawai, MD, PhD, Masami Bessho, MD, PhD,
Hiroshige Sato, MD, PhD, Toshihisa Asakura, MD, PhD,
Motonobu Nishimura, MD, PhD,
and Kenji Ikebuchi, MD, PhD

Department of Cardiovascular Surgery, Saitama Medical Center, and Departments of Cardiovascular Surgery, Cardiology, Hematology, and Transfusion and Cell Therapy, Saitama Medical School, Saitama, Japan

We describe a novel therapy of mononuclear cell transplantation combined with a left ventricular assist device (LVAD) for severe ischemic heart failure. Significant myocardial recovery by the LVAD rarely occurs in the severely failing heart. We undertook successful mononuclear cell transplantation in a patient who sustained an acute myocardial infarction that had resulted in the LVAD therapy. The heart regained good function after cell transplantation, and the LVAD was explanted 6 weeks later. These results suggest that this novel therapy could be an alternative to cardiac transplantation for severe ischemic heart failure.

(Ann Thorac Surg 2007;83:661–2)

The discovery of pluripotent stem cells in an adult has opened a novel clinical research field, regenerative medicine [1]. Many studies have demonstrated that bone-marrow-derived progenitor cells can differentiate into cardiomyocytes and endothelial cells, and they can be involved in repairing injured hearts [2]. Several clinical trials of autologous bone-marrow-derived mononuclear cell transplantation after acute myocardial infarction revealed the steady improvement in cardiac function [3]. We report a successful myocardial recovery with mononuclear cell transplantation and left ventricular assist device (LVAD) support after cardiogenic shock due to acute myocardial infarction.

A 61-year-old man who had diabetes mellitus was transferred in a shock state due to acute myocardial infarction. Emergency cardiac catheterization demonstrated the diagnosis of complete occlusion of the #7 left anterior descending artery (LAD) and 90% stenosis of the #2 right coronary artery (RCA). The culprit lesion, #7LAD, was not eligible for percutaneous coronary intervention because the wire could not cross it. Thereafter, the patient's shock state was worse, and percutaneous cardiopulmonary support was initiated.

Accepted for publication June 23, 2006.

Address correspondence to Dr Gojo, Department of Cardiovascular Surgery, Saitama Medical Center 1981 Kamoda, Kawagoe, Saitama 350-8550, Japan; e-mail: satoshi@saitama-med.ac.jp.

Despite maximum pharmacologic support, the patient lapsed into multiple organ failure. The decision was made implant a Toyobo LVAD (Toyobo, Inc, Osaka, Japan), and simultaneously perform a coronary artery bypass graft to the LAD and RCA with saphenous veins.

The status of multiple organ failure was gradually improved, but an ejection fraction (EF) by echocardiography was 0.13 on day 97 after LVAD implantation (Fig 1). Scintigraphy demonstrated complete infarctions in the anteroseptal and inferior walls (Fig 2). The patient was briefed in detail about mononuclear cell transplantation. This clinical study had been approved by the Ethics Committee of the Saitama Medical School, Saitama, Japan.

Bone marrow (600 mL) was aspirated under general anesthesia from both posterior ilia and enriched to the mononuclear cell fraction. The mononuclear cells were implanted in the infarcted zone through the saphenous grafts to the LAD and RCA on day 99 after LVAD implantation. During the procedure, the electrocardiogram was monitored and did not demonstrate any significant changes to suggest ischemic events. The possibility of microemboli was also negative on the basis of the stable normal values for creatine kinase-MB fraction and troponin-T after the procedure.

The patient's cardiac function became gradually better with time after the cell transplantation. The LVAD was removed on day 43 after mononuclear cell transplantation. The EF increased from 0.064 to .40 and remained stable, as assessed by echocardiography. Analysis of LV function by scintigraphy demonstrated a sustained improvement in blood perfusion and regional EF in the apical and inferior walls and growing thickness of the septal and inferior walls in the time course (Fig 2). The patient was discharged 58 days after explantation of the LVAD. After mononuclear cell transplantation, there were no complications, including acute inflammatory response, novel infarction, malignant arrhythmias, or ectopic differentiation.

Comment

Our aim was to extend the target of cell transplantation from the mild to the severely failing heart. The requirements were (1) a donor cell type, (2) an implantation procedure, including duration, route, and targets for cell delivery, and (3) a timing of cell transplantation after LVAD implantation. We chose bone-marrow-derived mononuclear cells to contain all of the cell fractions because (1) there is a controversy about the cell source to be grafted, (2) nobody can deny the possibility that the enrichment procedure will cause the useful cell population to be lost based on the current experimental data, and (3) pure, dense stem cells in a site might induce an ectopic differentiation.

As a grafting route, an antegrade intracoronary infusion through the saphenous vein grafts was chosen to avoid the isolated islet-like formation of grafted cells by direct injection into the myocardium, which could not effectively induce neogenesis of either cardiomyocytes or coronary capillaries.

The final important issue of the protocol was the timing of the cell transplantation after LVAD implantation. Although the LVAD improves cardiac milieu interne in the

Published by Elsevier Inc

0003-4975/07/$32.00
doi:10.1016/j.athoracsur.2006.06.074

Ann Thorac Surg
2007;83:661–2

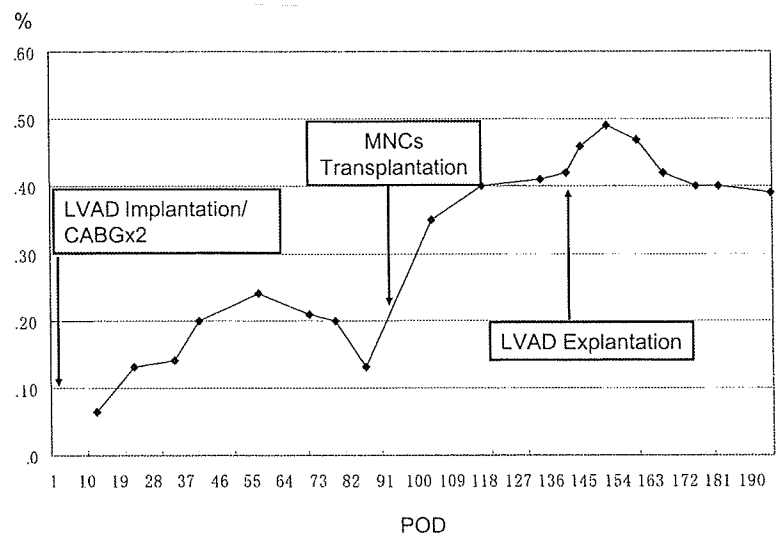

Fig 1. Left ventricular ejection fraction (EF) in transthoracic echocardiography. After left ventricular assist system (LVAS) inplantation, the first evaluation showed an EF of 6.4%. In the time course under LVAS support, EF gradually improved, but the value began decreasing 2 months later. (POD = postoperative day; CABG = coronary artery bypass grafting; MNCs = mononuclear cells; LVAD = left ventricular assist device.)

FEATURE ARTICLES

early phase, long-term LVAD support induces ventricular atrophy so that the LVAD is a double-edged sword. We had been examining EF, LV wall thickness, and motions by echocardiography. Because the decline of EF commenced on day 72 after LVAD implantation, we judged that the global effects of LVAD for cardiac recovery had turned from benefits to drawbacks and performed mononuclear cell transplantation on day 99 after LVAD implantation.

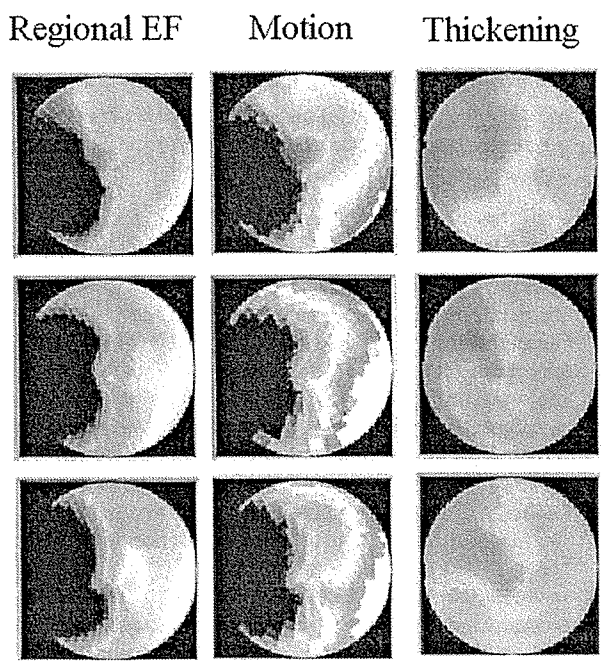

Fig 2. Technetium (Tc 99m)-tetrofosmin-gated single photon emission computed tomography. (Upper panels) Thirty-seven days after left ventricular assist device (LVAD) implantation and two coronary artery bypass grafts. (Middle panels) Twenty-nine days after mononuclear cell transplantation. (Lower panels) Twenty-five days after LVAD explantation (57 days after mononuclear cell transplantation).

The structural and functional improvements in last scintigraphy compared with that 1 month after mononuclear cell transplantation suggest that the cells engrafted, survived, and functioned in recipient heart. Grafted mononuclear cells release a wide array of cytokines related to the regeneration process. Mononuclear cell transplantation might stimulate the native environment to promote angiogenesis and cardiomyogenesis through the paracrine fashion in addition to vasculogenesis by the mononuclear cells themselves.

Many reports demonstrated that the LVAD support could induce reverse remodeling. In addition to relief of myocardium from the mechanical stretch of LVAD, the reverse remodeling of diseased heart could facilitate the engraftment, survival, and differentiation process of the grafted cells. Taken together, we think that mononuclear cell transplantation could fully work to repair the end-stage failing heart under the resting state created by LVAD support. This synergy effect of mononuclear cell transplantation and LVAD could be an explanation of this cardiac resurrection.

In conclusion, mononuclear cell transplantation for the treatment of ischemic cardiomyopathy with LVAD led to successful recovery of the failing heart and the LVAD to be unnecessary. We believe that this combination therapy might be an alternative to cardiac transplantation in the treatment of ischemic end-stage heart failure.

This work was supported in part by a Research Grant for Cardiovascular Diseases (16C-6) from the Ministry of Health, Labour and Welfare.

References

1. Pittenger MF, Mackay AM, Beck SC, et al. Multilineage potential of adult human mesenchymal stem cells. Science 1999;284:143–7.
2. Gojo S, Umezawa A. Plasticity of mesenchymal stem cells—regenerative medicine for diseased hearts. Hum Cell 2003;16:23–30.
3. Wollert KC, Meyer GP, Lotz J, et al. Intracoronary autologous bone-marrow cell transfer after myocardial infarction: the BOOST randomised controlled clinical trial. Lancet 2004;364:141–8.

Circ J 2006; **70:** 800–801

Stent Deformity Caused by Coronary Artery Spasm

Toshihiko Yoshida, MD; Yoshio Kobayashi, MD; Takashi Nakayama, MD; Nakabumi Kuroda, MD; Nobuyuki Komiyama, MD*; Issei Komuro, MD

Previous studies have shown that coronary stents have radial strength above the pressure induced by coronary artery spasm. This case report describes a stent deformity caused by coronary artery spasm during percutaneous coronary intervention. (*Circ J* 2006; **70:** 800–801)

Key Words: Angioplasty; Stent; Vasospasm

Despite full medical treatment with calcium channel blockers and nitrates, some patients with coronary artery spasm continue to have recurrent episodes of angina and myocardial infarction, and arrhythmic sudden death might occur[1–6] Previous reports demonstrate the usefulness of coronary stents to prevent vasospasm refractory to medical therapy[7–9] However, coronary stent implantation is sometimes ineffective in patients with multivessel spasm[10] This case report describes another limitation of coronary stent implantation to prevent coronary artery spasm.

Case Report

A 53-year-old man had been well until he had severe chest pain caused by acute myocardial infarction. He was referred 2 weeks after the onset of acute myocardial infarction. Coronary angiography revealed a 90% stenosis in the proximal obtuse marginal artery (Fig 1A). There was no significant stenosis in the left anterior descending coronary artery and right coronary artery. A 0.014-inch Skipper guidewire (Asahi Intecc, Nagoya, Japan) was placed across the lesion into the distal obtuse marginal artery. Predilation was performed by using a 3.0-mm OMNIPASS balloon catheter (Cordis, Miami, FL, USA) inflated to 6 atm. Intravascular ultrasound (IVUS) imaging was performed in the obtuse marginal artery using a 30-MHz 3.2F Ultracross catheter (Boston Scientific, Natick, MA, USA). The IVUS image showed a significant stenosis with fibrofatty plaque. A 25 mm NIR stent premounted on a 3.0-mm balloon catheter (Medinol, Tel Aviv, Israel) was deployed in the proximal obtuse marginal artery using an inflation pressure of 14 atm. Angiography and IVUS showed a good result (Figs 1B,2A). After the guidewire was withdrawn, the patient complained of chest pain; electrocardiogram demonstrated ST-segment elevation in lead I and aV_L and the systolic blood pressure dropped from 140 to 80 mmHg. Angiography demonstrated coronary artery spasm at the proximal stented segment and distal reference (Fig 1C). Thereafter, stent deformity was observed (Fig 2B). Intravenous norepinephrine (0.2 mg) and intracoronary nitroglycerine (200 μg) were administered. The systolic blood pressure increased to 100 mm Hg and the coronary artery spasm was relieved (Fig 1D). Further coronary intervention was not performed because there was no flow disturbance (TIMI 3) in the obtuse marginal artery. The patient received oral aspirin (100 mg daily), ticlopidine (100 mg twice daily for 4 weeks), diltiazem (100 mg daily), and isosorbide mononitrate (20 mg twice daily). There was no in-hospital event. During follow-up, no adverse event was observed. Six months later, follow-up angiography was performed. The deformed stent (Fig 2C) and a 25% stenosis at the distal stented segment (Fig 1E) were observed.

Discussion

Calcium antagonists and nitrates are effective in preventing coronary artery spasm in most cases. However, coronary artery spasm refractory to the treatment with these drugs is observed in some cases[1–6] Alpha-1 blocking agents[2] magnesium[3] benzhexol hydrochloride[4] denopamine[5] and nicorandil[6] have been reported as alternatives. Previous reports demonstrated the efficacy of coronary stenting in patients with clinically severe coronary artery spasm refractory to aggressive pharmacologic management[7–9] Gaspardone et al evaluated the usefulness of coronary stent placement in 9 patients with vasospastic angina refractory to medical treatment[10] The NIR stent was used in 6 patients. During follow-up, 3 patients developed recurrent episodes of angina at rest. Holter monitoring demonstrated ST-segment elevation associated with angina. Repeat coronary angiography showed coronary artery spasm after the administration of methylergometrine in these patients. Coronary artery spasm occurred proximally to the previously implanted stent in 2 patients and in other coronary arteries in 1 patient.

Coronary artery spasm is sometimes observed during percutaneous coronary intervention. It is usually relieved by the intracoronary administration of nitroglycerin. Balloon inflation at a low pressure may be used to treat it. Agrawal et al calculated the minimum acceptable collapse pressure for stents using arterial strain caused by experimentally induced artery spasm[11] They reported 0.4 atm as the minimum acceptable limit for collapse pressure. Almost all coronary stents have more radial strength[12,13] The NIR stent is one of the stents with strong radial strength[12] An in-vitro study reported that the NIR stent expanded to 3 mm

(Received January 10, 2006; revised manuscript received March 10, 2006; accepted March 28, 2006)

*Department of Cardiovascular Science and Medicine, Chiba University Graduate School of Medicine, Chiba, *Division of Cardiovascular Medicine, Saitama Medical College, Saitama, Japan*
Mailing address: Yoshio Kobayashi, MD, Department of Cardiovascular Science and Medicine, Chiba University Graduate School of Medicine, 1-8-1 Inohana, Chuo-ku, Chiba 260-8670, Japan. E-mail: yoshio.kobayashi@wonder.ocn.ne.jp

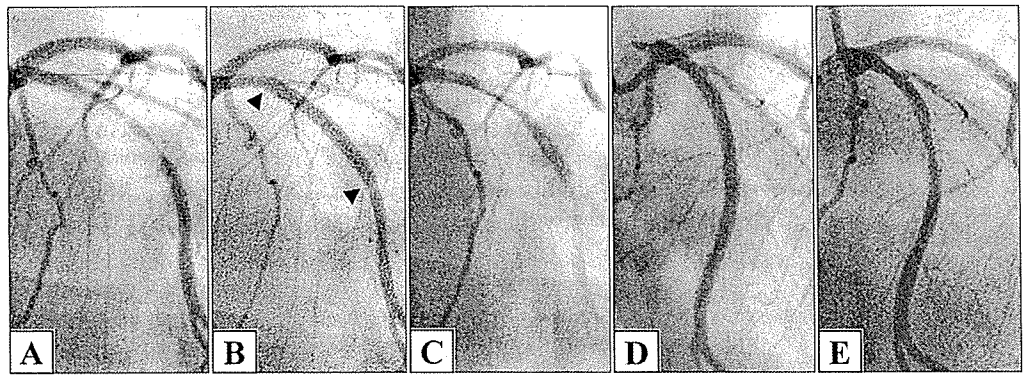

Fig 1. Coronary angiography showing a 90% stenosis in the proximal obtuse marginal artery (A). After deployment of a NIR stent, angiography demonstrates a good result (B). Arrowheads indicate the edges of the stent. Angiography demonstrates coronary artery spasm at the proximal stented segment and distal reference (C). After intracoronary administration of nitroglycerine, coronary artery spasm is relieved (D). Follow-up angiography shows a 25% stenosis at the distal stented segment (E).

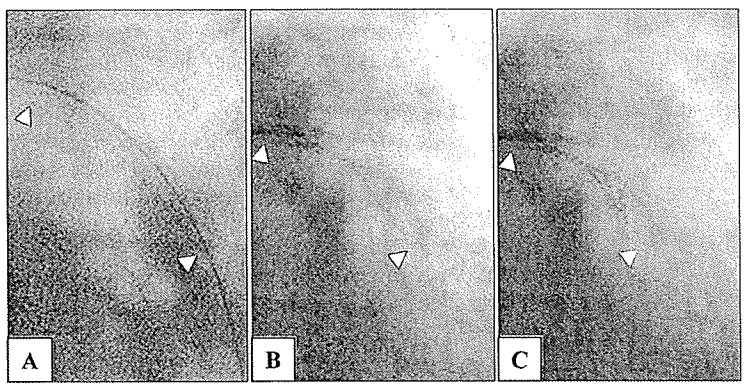

Fig 2. Fluoroscopy demonstrates a fully expanded stent (A). After coronary artery spasm, stent deformity is observed (B). Fluoroscopy shows the deformed stent at follow up (C). Arrowheads indicate the edges of the stent.

collapsed at a compressive strength of 1.05 atm.[12] This case report demonstrates unusually severe coronary artery spasm because the NIR stent was deformed. Coronary stenting may be ineffective in some patients with severe coronary artery spasm as well as in those with multivessel spasm. These are the limitations of stent implantation for coronary artery spasm. Thus, alternative medical treatment such as α-1 blocking agents[2] magnesium[3] benzhexol hydrochloride[4] denopamine[5] and nicorandil[6] should be tried for coronary artery spasm refractory to calcium antagonists and nitrates before stent implantation is considered. Stent implantation would be the last resort. In some patients, stent implantation for refractory coronary artery spasm might be performed. However, intensive medical treatment should be continued in those patients even after stent implantation.

References

1. Takagi S, Goto Y, Hirose E, Terashima M, Sakuragi S, Suzuki S, et al. Successful treatment of refractory vasospastic angina with corticosteroids: Coronary arterial hyperactivity caused by local inflammation? *Circ J* 2004; **68:** 17–22.
2. Tzivoni D, Keren A, Benhorin J, Gottlieb S, Atlas D, Stern S. Prazosin therapy for refractory variant angina. *Am Heart J* 1983; **105:** 262–266.
3. Miyagi H, Yasue H, Okumura K, Ogawa H, Goto K, Oshima S. Effect of magnesium on anginal attack induced by hyperventilation in patients with variant angina. *Circulation* 1989; **79:** 597–602.
4. Joy M, Haywood GA, Webb-Peploe MM. Management of a case of refractory variant angina with benzhexol hydrochloride (trihexyphenidyl hydrochloride). *Br Heart J* 1985; **54:** 448–451.
5. Shimizu H, Lee JD, Ogawa KB, Sugiyama T, Yamamoto M, Hara A, et al. Refractory variant angina relieved by denopamine. *Jpn Circ J* 1991; **55:** 692–694.
6. Noguchi T, Nonogi H, Yasuda S, Daikoku S, Morii I, Itoh A, et al. Refractory coronary spasm relieved by intracoronary administration of nicorandil. *Jpn Circ J* 2000; **64:** 396–398.
7. Lopez JA, Angelini P, Leachman DR, Lufschanowski R. Gianturco-Roubin stent placement for variant angina refractory to medical treatment. *Cathet Cardiovasc Diagn* 1994; **33:** 161–165.
8. Nakamura T, Furukawa K, Uchiyama H, Seo Y, Okuda S, Ebizawa T. Stent placement for recurrent vasospastic angina resistant to medical treatment. *Cathet Cardiovasc Diagn* 1997; **42:** 440–443.
9. Kultursay H, Can L, Payzin S, Turkoglu C, Altintig A, Akin M, et al. A rare indication for stenting: Persistent coronary artery spasm. *Heart Vessels* 1996; **11:** 165–168.
10. Gaspardone A, Tomai F, Versaci F, Ghini AS, Polisca P, Crea F, et al. Coronary artery stent placement in patients with variant angina refractory to medical treatment. *Am J Cardiol* 1999; **84:** 96–98.
11. Agrawal CM, Haas KF, Leopold DA, Clark HG. Evaluation of poly (L-lactic acid) as a material for intravascular polymeric stents. *Biomaterials* 1992; **13:** 176–182.
12. Schrader SC, Beyar R. Evaluation of the compressive mechanical properties of endoluminal metal stents. *Cathet Cardiovasc Diagn* 1998; **44:** 179–187.
13. Rieu R, Barragan P, Masson C, Fuseri J, Garitey V, Silvestri M, et al. Radial force of coronary stents: A comparative analysis. *Catheter Cardiovasc Interv* 1999; **46:** 380–391.

ELSEVIER

International Journal of Cardiology 109 (2006) 430 – 431

International Journal of Cardiology

www.elsevier.com/locate/ijcard

Letter to the Editor

Endocardial fibrosis in subacute non-Q wave myocardial infarction demonstrated by multislice computed tomography

Nobusada Funabashi*, Nobuyuki Komiyama, Miki Asano, Issei Komuro

Department of Cardiovascular Science and Medicine, Chiba University Graduate School of Medicine, 1-8-1 Inohana, Chuo-ku, Chiba City, Chiba 260-8670, Japan

Received 24 March 2005; accepted 1 April 2005
Available online 10 May 2005

Keywords: Endocardial fibrosis; Subacute non Q-wave myocardial infarction; Multislice computed tomography

Several diagnostic modalities such as echocardiography [1], magnetic resonance imaging (MRI) [2], single photon emission computed tomography (SPECT) [3], and positron emission tomography (PET) [4], can be used to evaluate infarcted myocardium. However, it is difficult to accurately distinguish the location of the infarct in the myocardium, such as in non-Q wave myocardial infarction (MI), which suggests an endocardial MI rather than a transmural MI.

A 57-year-old man had an anteroseptal MI 15 years ago. Recently, he had a second MI with new ST segment depressions and inverted T waves on ECG in the lateral precardial leads. Conventional coronary angiograms revealed complete occlusion of the proximal portion of the LAD and the collateral branches to the peripheral arteries of the LAD from the left circumflex branch (Fig. 1). The proximal portion of the obtuse marginal (OM) branch was totally occluded. The peripheral portion of the OM was observed by blood flow from the collateral arteries from the posterior lateral branch. We were unable to determine which arteries were responsible for the infarction from the angiographic data.

To clarify the location of the non-Q wave infarct site, enhanced ECG gated multislice computed tomography (CT) (Aquilion, Toshiba) was performed with a 1-mm slice thickness and a helical pitch of 1.0. Routine scanning was performed with intravenous injection of 100ml of iodinated contrast material (300 mg I/ml), at 30 s and 7 min after the injection. The CT revealed late enhancement of the endocardial portion of the lateral apex of the left ventricle, which were hypodense in the early phase (arrows, Fig. 2). This region still exhibited normal myocardial thickness at the epicardial site. This indicated that reconstruction of the interstitium, possibly fibrotic changes, had occurred in this region. Endocardial fibrotic changes observed by CT with the findings of the

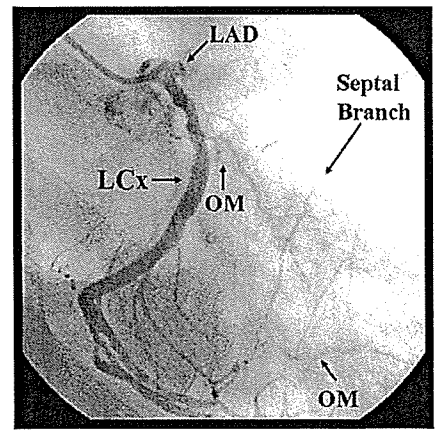

Fig. 1. Conventional coronary angiogram revealed an occlusion of the proximal portion of the left anterior descending branch (LAD) and the collateral branches to the peripheral arteries of the LAD through the septal branches from the left posterior descending branch. The proximal portion of the obtuse marginal branch (OM) was totally occluded (arrowhead) and the peripheral branch of OM was observed by the collateral flow from the posterior lateral branch. LCx, left circumflex branch.

* Corresponding author.
E-mail address: nobusada@ma.kcom.ne.jp (N. Funabashi).

0167-5273/$ - see front matter
doi:10.1016/j.ijcard.2005.04.013

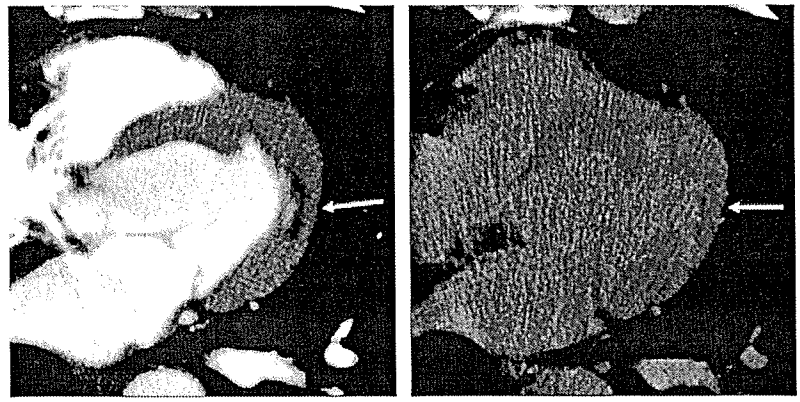

Fig. 2. Axial source images of electrocardiogram-gated multislice computed tomography (CT) from end-diastole in the early (A) and late (B) phases after injection of the contrast material. The endocardial portion of the lateral apex of the left ventricle revealed hypodense CT values during the early phase after the injection of the contrast material (arrows). Normal myocardial thickness at the epicardial site was still evident and enhancement occurred only in the late phase. This area consisted of interstitial changes such as fibrosis or edema and appeared not to be transmural, since this region still exhibited normal myocardial thickness at the epicardial site with isodense CT values that were the same as seen on images of other normal myocardia.

ECG and coronary angiograms suggested that the culprit coronary artery in this event must be the OM.

Detection of the location of an endocardial infarct in the myocardium is difficult, as non Q wave MI frequently occurs in subjects with multi-vessel disease of the coronary arteries, and thus, it may be difficult to distinguish the responsible vessels causing non Q wave MI. Therefore, it is very important to clearly distinguish the location of the infarct area as transmural or localized in the endocardium. Such diagnosis may help to prepare a strategy for percutaneous transmural coronary intervention.

ECG-gated multislice CT has a better spatial resolution than MRI, SPECT, and PET [5], and using characteristics of iodinated contrast material, which shows defect in the early phase and abnormal enhancement in the late phase in myocardial fibrosis [6], it is possible to detect the location of the endocardial fibrosis, which helps to determine which arteries are responsible for the infarction.

References

[1] Park SW, Lee SY, Park SJ, Lee SC, Gwon HC, Kim DK. Quantitative assessment of infarct size in vivo by myocardial contrast echocardiography in a murine acute myocardial infarction model. Int J Cardiol 2004;97(3):393–8.

[2] Ogawa E, Okinaka T, Motoyasu M, et al. A case of acute myocardial infarction caused by left main trunk disease with dilated cardiomyopathy. Int J Cardiol 2005;98(3):507–8.

[3] Fiorina P, Pattoneri P, Paganelli C, Secchi A, Calbiani B, Astorri E. Correlation between non-reversible thallium-201 myocardial perfusion defect and ECG criteria in the diagnosis of apical myocardial infarction. Int J Cardiol 2004;95(2–3):251–4.

[4] Yoshida K, Gould KL. Quantitative relation of myocardial infarct size and myocardial viability by positron emission tomography to left ventricular ejection fraction and 3-year mortality with and without revascularization. J Am Coll Cardiol 1993;22(4):984–97.

[5] Ratti C, Barbieri A, Ligabue G, et al. Non-invasive, three-dimensional visualization of coronary artery bypass grafts by multislice spiral computed tomography. Int J Cardiol 2005;99(1):157–9.

[6] Masuda Y, Yoshida H, Morooka N, Watanabe S, Inagaki Y. The usefulness of X-ray computed tomography for the diagnosis of myocardial infarction. Circulation 1984;70(2):217–25.

Location of Focal Vasospasm Provoked by Ergonovine Maleate Within Coronary Arteries in Patients With Vasospastic Angina Pectoris

Tomomi Koizumi, MD, PhD[a], Masaki Yokoyama, MD, PhD[b], Susumu Namikawa, MD, PhD[b], Nehiro Kuriyama, MD, PhD[b], Mizuo Nameki, MD, PhD[b], Takashi Nakayama, MD[b], Hideaki Kaneda, MD, PhD[a], Krishnankutty Sudhir, MD, PhD[a], Paul G. Yock, MD[a], Nobuyuki Komiyama, MD, PhD[c], and Peter J. Fitzgerald, MD, PhD[a,*]

This study examined whether coronary focal vasospasm occurs in a nonuniform distribution within the coronary tree and whether a longitudinal plaque distribution pattern is present in patients with vasospastic angina using 3-dimensional intravascular ultrasound analysis. Of 121 patients with clinically suspected angina without fixed stenosis in the coronary arteries, vasospasm was provoked in 82 patients with 92 lesions (42 focal, 50 diffuse) by intravenous ergonovine maleate injection. Most focal vasospasms occurred in the proximal third of the coronary arteries (proximal 28, mid 8, distal 6, $p < 0.01$), corresponding to the historical high-risk zones for acute coronary occlusion. More plaque burden also existed in the proximal third of the coronary arteries in patients with focal vasospasm. (Am J Cardiol 2006;97:1322–1325)

Vasospasm in coronary arteries has been shown to play an important role in the pathogenesis of not only variant angina, but also acute myocardial infarction, fatal arrhythmia, and sudden cardiac death.[1–3] Focal vasospasm has been associated with a significantly higher incidence of cardiac events than diffuse vasospasm.[4] A recent report has shown that acute coronary occlusions tend to cluster in a predictable high-risk zone within the proximal third of the coronary arteries.[5] However, the geographic evaluation of the site of focal vasospasm in the coronary artery has not been fully elucidated. Moreover, the longitudinal plaque distribution pattern has not been examined in patients with vasospastic angina using 3-dimensional intravascular ultrasound (IVUS) analysis.

• • •

Provocation of vasospasm by intravenous ergonovine maleate administration was performed in 121 patients with clinically suspected angina, without fixed stenosis in the coronary arteries, after admission to the Center for Cardiovascular Interventions, Chiba University Hospital, Chiba, Japan. After the patients provided informed consent, cardiac catheterization, coronary angiography, and a subsequent coronary vasospasm provocation test were performed as a part of the diagnostic procedure. All medications, except for emergency sublingual nitroglycerin, were discontinued ≥24 hours before cardiac catheterization. After administration of diazepam 5 mg for sedation, patients were taken to the catheterization laboratory. Any drugs likely to affect coronary hemodynamics were not used during the catheterization procedure before selective coronary angiography. Standard cardiac catheterization, including pressure recording, left ventriculography, and selective coronary angiography, was performed after intravenous injection of 2,000 to 3,000 U of heparin.

After confirmation of no luminal narrowing of >50% in the coronary artery by control coronary angiography, 0.2 mg of ergonovine maleate was administrated intravenously to provoke vasospasm. A standard 12-lead electrocardiogram was used for monitoring during coronary angiography to detect any ST-T segment changes. Immediately after chest pain with ST-T segment elevation or ST depression of >0.1 mV was observed or 3 minutes after ergonovine maleate was injected, coronary angiography was performed to confirm the provocation of vasospasm. Subsequently, 100 to 200 μg of intracoronary nitroglycerin was injected to relieve the vasospasm. Coronary angiography and intracoronary injection of nitroglycerin were repeated until the coronary vasospasm was completely relieved.

Of the 92 lesions in 82 patients with positive results, 42 had focal vasospasm, defined as a discrete transient narrowing of >90% that was localized to coronary arteries and associated with ST-T segment elevation or depression of >0.1 mV by 12-lead electrocardiography. The remaining 50 lesions were classified as nonfocal (i.e., diffuse vasoconstriction or diffuse vasospasm) that was diagnosed when a transient vessel narrowing of >90% compared with the control coronary angiogram was observed from the proximal to distal segment in the 3 major coronary arteries, with

[a]Center for Research in Cardiovascular Interventions, Division of Cardiovascular Medicine, Stanford University, Stanford, California; [b]Center for Cardiovascular Interventions, Chiba University Hospital, Chiba; and [c]Division of Cardiology, Saitama Medical School, Saitama, Japan. Manuscript received August 31, 2005; revised manuscript received and accepted November 15, 2005.

* Corresponding author: Tel: 650-498-6034; fax: 650-498-6027.
E-mail address: ivus@crci.stanford.edu (P.J. Fitzgerald).

0002-9149/06/$ – see front matter
doi:10.1016/j.amjcard.2005.11.073

Table 1
Clinical characteristics

Variable	Spasm Type		p Value
	Diffuse (n = 47)	Focal (n = 35)	
Age (yrs)	58.6 ± 6.2	56.3 ± 9.8	0.19
Men	26 (55%)	29 (83%)	<0.01
Smoker	21 (45%)	18 (51%)	0.55
Diabetes mellitus	5 (11%)	3 (9%)	0.76
Hypertension*	7 (15%)	3 (9%)	0.38
Hypercholesterolemia†	19 (40%)	5 (14%)	0.01

Data are presented as mean ± SD or numbers (percentages).

* Defined as use of antihypertensive therapy or systolic blood pressure >140 mm Hg.

† Defined as fasting total cholesterol level >220 mg/dl or use of lipid-lowering therapy.

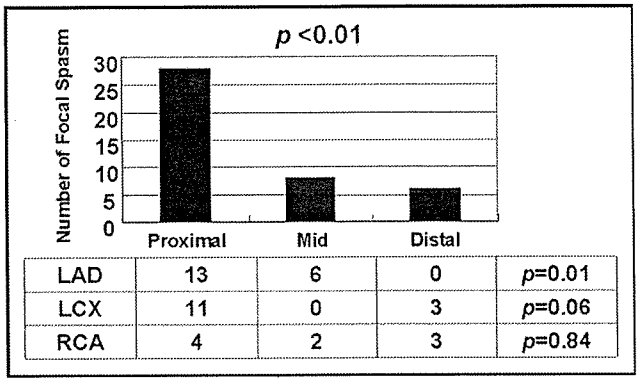

LAD	13	6	0	p=0.01
LCX	11	0	3	p=0.06
RCA	4	2	3	p=0.84

Figure 1. Site distribution of focal vasospasm in epicardial coronary tree. Overall, focal vasospasm clustered within the proximal third of the coronary artery (proximal 28, mid 8, distal 6, p <0.01). Sites of focal vasospasm in the left anterior descending artery (LAD; proximal 13, mid 6, distal 0, p = 0.01) and left circumflex artery (LCX; proximal 11, mid 0, distal 3, p = 0.06) were nonuniform. In contrast, sites of focal vasospasm in the right coronary artery (RCA) were uniform (proximal 4, mid 2, distal 3, p = 0.84).

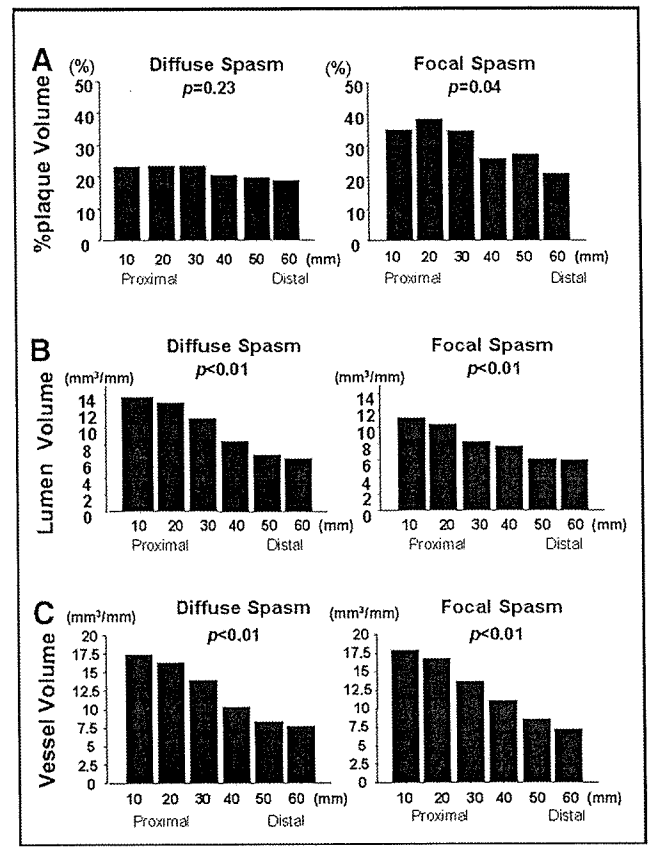

Figure 2. *(A)* Distribution of percentage of plaque volume in each 10-mm section from ostium to 60 mm distally of coronary artery. *Left*, diffuse vasospasm. Uniform distribution of percentage of plaque volume (p = 0.23). *Right*, focal vasospasm. Nonuniform distribution of percentage of plaque volume (p = 0.04) predominantly in proximal 30 mm. *(B, C)* Distribution of lumen volume and vessel volume in each 10-mm section from ostium to 60 mm distally of coronary artery. In diffuse and focal vasospasm, lumen volume and vessel volume tapered significantly from the ostium to 60 mm distally (p <0.01).

or without discrete changes in the coronary diameter in the small branches, in association with ST elevation or depression of >0.1 mV by 12-lead electrocardiography. Transient vasoconstriction of >25% compared with the control angiogram after administration of ergonovine maleate was considered a negative test finding.

The site of focal vasospasm in each epicardial coronary artery was classified into 3 locations (proximal, mid, or distal) according to the coronary artery map from the American Heart Association classification.[6]

In a subset of 26 patients, IVUS was performed to examine the longitudinal plaque distribution pattern in patients with vasospastic angina, using a 2.9-Fr, 40-MHz, single-element, mechanical ultrasound catheter (Boston Scientific, Natick, Massachusetts) with motorized pull-back devices (0.5 mm/s). Per protocol, intracoronary nitroglycerin was injected before image acquisition. Twenty-two IVUS images could be recorded from the coronary artery ostium to a distance of >60 mm distally on s-VHS videotape for off-line analysis. Three-dimensional reconstruction of the IVUS images was performed using a commercially available quantitative analysis system, which runs on an Intel Pentium-based personal computer system with Windows NT (echoPlaque, version 2.9, INDEC Systems, Mountain View, California). After digitization of the IVUS recordings at a frame rate of 15 images/s, longitudinal views of the studied segments were automatically processed by the system. The lumen and external elastic membrane areas were manually delineated from the ostium to a distance of >60 mm distally at 16-frame intervals, and the interpolated measurements of the remaining frames were automatically generated. Using Simpson's method, the lumen volume and vessel volume inside the external elastic membrane were calculated. The percentage of plaque volume of each 10 mm from the ostium to 60 mm distally of the coronary artery was obtained with the following formula: ([vessel volume − lumen volume]/vessel volume) × 100.

The means ± SDs are presented for continuous data. The chi-square test was used to compare the categorical vari-

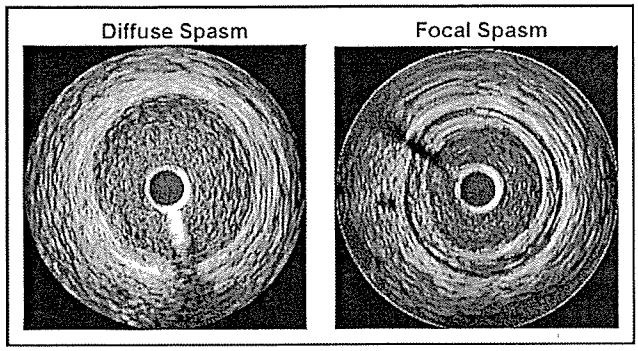

Figure 3. *Left*, Cross-sectional IVUS image at site of diffuse vasospasm in proximal left anterior descending coronary artery showing no intima-media thickening (i.e., normal appearance). *Right*, cross-sectional image of site of focal vasospasm in proximal left anterior descending coronary artery showing concentric intima-media thickening with qualitatively fibrofatty tissue.

ables. Analysis of variance was used to test whether the locations of focal vasospasm and plaque burden were uniformly distributed in the coronary arteries. A p value of <0.05 was considered statistically significant.

The demographic data are reported in Table 1. In this study, the prevalence of coronary risk factors was comparable between the patients with focal and diffuse vasospasms, except that the group with focal vasospasm had more men ($p < 0.01$) and less frequent hypercholesterolemia ($p = 0.01$), defined as a fasting total cholesterol level of >220 mg/dl or the use of lipid-lowering therapy.

Overall, the site of focal vasospasm was clustered within the proximal third of the coronary arteries ($p < 0.01$; Figure 1). The site of focal vasospasm in the left anterior descending artery ($p = 0.01$) and left circumflex artery ($p = 0.06$) was nonuniform, despite uniform distribution in the right coronary artery ($p = 0.84$). Plaque was distributed nonuniformly in the proximal third of the coronary arteries in patients with focal vasospasm ($n = 10$, $p = 0.04$), although plaque was distributed uniformly in patients with diffuse vasospasm ($n = 12$, $p = 0.23$). The lumen and vessel area tapered similarly in the 2 groups (Figure 2). Cross-sectional IVUS images at the site of vasospasm in the proximal left anterior descending artery are shown in Figure 3.

• • •

Schroeder et al[7] first described focal and nonfocal coronary arterial spasm during administration of ergonovine maleate in 1977. They had already recognized that these 2 patterns of vasospasm typically have a different appearance on angiography.[7] After that, some investigators demonstrated the pathophysiology of coronary spasm, especially of focal vasospasm. Heupler[8] suggested that even in the absence of angiographic disease, occult atherosclerotic lesions could be present at the sites of focal coronary spasm. This finding was proved by IVUS studies showing minimal atherosclerotic lesions at the site of focal spasm.[9] Coronary focal spasm is caused by local hyperreactivity to a generalized constrictor stimulus on minimal atherosclerosis.[10] Also, at the site of focal vasospasm, erosion, ulcer, or thrombus was detected by coronary angioscopy in locally injured coronary arteries.[11] From a prognostic viewpoint of vasospastic angina, focal vasospasm has been associated with a significantly higher incidence of cardiac events, including sudden death, myocardial infarction, and unstable angina, than diffuse vasospasm.[4]

Under these clinical conditions, previous studies have suggested that focal vasospasm might be associated with more advanced atherosclerosis than diffuse vasospasm in patients with vasospastic angina. Thus, providing a complete longitudinal view of plaque inside the vessel to better evaluate the site of focal vasospasm within the coronary artery would benefit our understanding of this clinical situation.

A recent report has shown that acute coronary thrombotic occlusions (due to plaque rupture) leading to ST-elevation myocardial infarction are clustered within the proximal third of the coronary arteries.[5] Also, most vulnerable plaques occur predominantly in the proximal portion of the 3 major coronary arteries.[12] Furthermore, Hong et al,[13] using IVUS, found that plaque ruptures occurred mainly in the proximal segments of the left anterior descending artery (83% of the plaque ruptures were 10 to 40 mm from the ostium) and the proximal and distal segments of the right coronary artery (48% of the plaque ruptures were 10 to 40 mm from the ostium and 32% of the plaque ruptures were >70 mm from the ostium). These data are similar to our results that focal spasm occurred mainly in the proximal (68%) segment of the left anterior descending artery and the proximal (44%) and distal (33%) segments of the right coronary artery. Considering that plaque ruptures represent only 2/3 of the causes of coronary thrombosis,[14,15] focal coronary spasm and plaque rupture may play an important role in the pathogenesis of acute myocardial infarction, respectively, or simultaneously. Additional research is needed to examine the contribution of focal vasospasm to plaque rupture at these sites.

We have also shown that an increased plaque burden exists in the proximal third of the coronary arteries in patients with focal vasospasm using 3-dimensional IVUS analysis. This plaque accumulation might progress and represent a vulnerability to plaque rupture, leading to acute coronary occlusion.[16] Because the lumen areas tapered similarly in the 2 groups, angiography could not reveal the plaque accumulation in the proximal segments of the coronary arteries. Taking into account the results that acute myocardial infarctions occur frequently in angiographically normal-looking segments,[17] IVUS may be a useful tool for detecting plaque severity.

Acknowledgment: We thank Heidi N. Bonneau, RN, MS, for her expert review of the manuscript.

1. Myerburg RJ, Kessler KM, Mallon SM, Cox MM, deMarchena E, Interian A Jr, Castellanos A. Life-threatening ventricular arrhythmias in patients with silent myocardial ischemia due to coronary-artery spasm. *N Engl J Med* 1992;326:1451–1455.
2. Roberts WC, Curry RC Jr, Isner JM, Waller BF, McManus BM, Mariani-Constantini R, Ross AM. Sudden death in Prinzmetal's angina with coronary spasm documented by angiography: analysis of three necropsy patients. *Am J Cardiol* 1982;50:203–210.
3. Suzuki H, Kawai S, Aizawa T, Kato K, Sunayama S, Okada R, Yamaguchi H. Histological evaluation of coronary plaque in patients with variant angina: relationship between vasospasm and neointimal hyperplasia in primary coronary lesions. *J Am Coll Cardiol* 1999;33: 198–205.
4. Mori F, Uchida T, Byun T, Tanino S, Imamura K, Oomori H, Nagashima M, Enta K, Tanaka M, Kasahara S, Hirosawa K. Cardiac events in vasospastic angina: site and morphology of coronary artery spasm is related to the long-term prognosis of vasospastic angina. *J Cardiol* 1999;33:191–199.
5. Wang JC, Normand SL, Mauri L, Kuntz RE. Coronary artery spatial distribution of acute myocardial infarction occlusions. *Circulation* 2004;110:278–284.
6. Austen WG, Edwards JE, Frye RL, Gensini GG, Gott VL, Griffith LS, McGoon DC, Murphy ML, Roe BB. A reporting system on patients evaluated for coronary artery disease: report of the Ad Hoc Committee for Grading of Coronary Artery Disease, Council on Cardiovascular Surgery, American Heart Association. *Circulation* 1975;51:5–40.
7. Schroeder JS, Bolen JL, Quint RA, Clark DA, Hayden WG, Higgins CB, Wexler L. Provocation of coronary spasm with ergonovine maleate: new test with results in 57 patients undergoing coronary arteriography. *Am J Cardiol* 1977;40:487–491.
8. Heupler FA Jr. Syndrome of symptomatic coronary arterial spasm with nearly normal coronary arteriograms. *Am J Cardiol* 1980;45:873–881.
9. Yamagishi M, Miyatake K, Tamai J, Nakatani S, Koyama J, Nissen SE. Intravascular ultrasound detection of atherosclerosis at the site of focal vasospasm in angiographically normal or minimally narrowed coronary segments. *J Am Coll Cardiol* 1994;23:352–357.
10. Kaski JC, Maseri A, Vejar M, Crea F, Hackett D. Spontaneous coronary artery spasm in variant angina is caused by a local hyperreactivity to a generalized constrictor stimulus. *J Am Coll Cardiol* 1989;14: 1456–1463.
11. Etsuda H, Mizuno K, Arakawa K, Satomura K, Shibuya T, Isojima K. Angioscopy in variant angina: coronary artery spasm and intimal injury. *Lancet* 1993;342:1322–1324.
12. Narula J, Finn AV, Demaria AN. Picking plaques that pop. *J Am Coll Cardiol* 2005;45:1970–1973.
13. Hong MK, Mintz GS, Lee CW, Lee BK, Yang TH, Kim YH, Song JM, Han KH, Kang DH, Cheong SS, et al. The site of plaque rupture in native coronary arteries: a three-vessel intravascular ultrasound analysis. *J Am Coll Cardiol* 2005;46:261–265.
14. Farb A, Burke AP, Tang AL, Liang TY, Mannan P, Smialek J, Virmani R. Coronary plaque erosion without rupture into a lipid core: a frequent cause of coronary thrombosis in sudden coronary death. *Circulation* 1996;93:1354–1363.
15. Burke AP, Farb A, Malcom GT, Liang YH, Smialek J, Virmani R. Coronary risk factors and plaque morphology in men with coronary disease who died suddenly. *N Engl J Med* 1997;336:1276–1282.
16. Nobuyoshi M, Tanaka M, Nosaka H, Kimura T, Yokoi H, Hamasaki N, Kim K, Shindo T, Kimura K. Progression of coronary atherosclerosis: is coronary spasm related to progression? *J Am Coll Cardiol* 1991;18:904–910.
17. Nissen SE, Yock P. Intravascular ultrasound: novel pathophysiological insights and current clinical applications. *Circulation* 2001;103:604–616.

Int J Cardiovasc Imaging
DOI 10.1007/s10554-007-9212-1

ORIGINAL PAPER

Quantitative colorimetry of atherosclerotic plaque using the L*a*b* color space during angioscopy for the detection of lipid cores underneath thin fibrous caps

Fumiyuki Ishibashi · Shinya Yokoyama · Kengo Miyahara · Alexandra Dabreo · Eric R. Weiss · Mark Iafrati · Masamichi Takano · Kentaro Okamatsu · Kyoichi Mizuno · Sergio Waxman

Received: 24 November 2006 / Accepted: 31 January 2007

Abstract
Objectives Yellow plaques seen during angioscopy are thought to represent lipid cores underneath thin fibrous caps (LCTCs) and may be indicative of vulnerable sites. However, plaque color assessment during angioscopy has been criticized because of its qualitative nature. The purpose of the present study was to test the ability of a quantitative colorimetric system to measure yellow color intensity of atherosclerotic plaques during angioscopy and to characterize the color of LCTCs.
Methods Using angioscopy and a quantitative colorimetry system based on the L*a*b* color space [L* describes brightness (–100 to +100), b* describes blue to yellow (–100 to +100)], the optimal conditions for measuring plaque color were determined in three flat standard color samples and five artificial plaque models in cylinder porcine carotid arteries. In 88 human tissue samples, the colorimetric characteristics of LCTCs were then evaluated.
Results In in-vitro samples and ex-vivo plaque models, brightness L* between 40 and 80 was determined to be optimal for acquiring b* values, and the variables unique to angioscopy in color perception did not impact b* values after adjusting for brightness L* by manipulating light or distance. In ex-vivo human tissue samples, b* value ≥23 (35.91 ± 8.13) with L* between 40 and 80 was associated with LCTCs (fibrous caps <100 μm).
Conclusions Atherosclerotic plaque color can be consistently measured during angioscopy with quantitative colorimetry. High yellow color intensity, determined by this system, was associated with LCTCs. Quantitative colorimetry during angioscopy may be used for detection of LCTCs, which may be markers of vulnerability.

Keywords Angioscopy · Quantitative colorimetry · Atherosclerotic plaque · Imaging

F. Ishibashi · A. Dabreo · E. R. Weiss · S. Waxman
Center for Translational Cardiovascular Research, Tufts New England Medical Center, Boston, MA, USA

S. Yokoyama · M. Takano · K. Okamatsu · K. Mizuno
Department of Internal Medicine, Chiba-Hokusoh Hospital, Nippon Medical School, Chiba, Japan

K. Miyahara
Institute of Archaeological Research Kyoto, Kyoto, Japan

M. Iafrati
Department of Vascular Surgery, Tufts New England Medical Center, Boston, MA, USA

S. Waxman (✉)
Lahey Clinic Medical Center, 41 Mall Road, Burlington, MA 01805, USA
e-mail: sergio.waxman@lahey.org

Abbreviations

ACS	Acute coronary syndromes
A/D	Analog to digital
CCD	Charge-coupled device
CIE	International Committee on Illumination
HIS	Hue, saturation, intensity
LCTC	Lipid core underneath thin fibrous cap
NTSC	National Television System Committee
POI	Point of interest
RGB	Red, green, blue
ROI	Region of interest
SD	Standard deviation

Introduction

Lipid cores underneath thin fibrous caps (LCTCs) are found in most ruptured plaques and a majority of culprit lesions of acute coronary syndromes (ACS) [1], and are thought to be the regions which may be vulnerable to thrombosis. Early detection of such regions may potentially lead to prediction and prevention of ACS [2]. LCTCs may appear yellow by angioscopy, based on the association of yellow plaque color with lipid-rich atheromas [3] or thin fibrous caps covering lipid cores [4], as well as clinical studies demonstrating the association of yellow lesions and ACS and thrombus [5–7]. However, use of yellow plaque color by angioscopy as a marker of LCTCs has been limited because of the qualitative nature of color measurement [8].

Lehmann et al. [9] studied quantitative colorimetry during angioscopy using two color coordinates and HSI (hue, saturation, intensity) color space (see http://www.en.wikipedia.org/wiki/HSL_color_space), and utilized it to differentiate thrombus based on color [10]. However, this system was not used to distinguish atherosclerotic plaques, which have a different range of color from thrombus. Miyamoto et al. [11] found an inverse relationship between yellow color saturation and the cap thickness of fibroatheromas. In their system, yellow saturation, derived from HSI color space, was used to represent yellow color intensity of plaques (see, http://www.en.wikipedia.org/wiki/Saturation_%28 color_theory%29). However, yellow saturation may not ideally represent the gradations of yellow color intensity because of its non-linear nature. In addition, the detailed process of optimization against the effect of variables unique to angioscopy was not examined in their system.

The International Committee on Illumination (CIE) 1976 color difference formula (L*a*b* color space) has been widely used to describe all the colors visible to the human eye (see, http://www.en.wikipedia.org/wiki/Lab_color_space). In this color space, yellow color intensity and brightness can be represented simply as positive b* and L* values. Because of its linear nature, quantitative colorimetry using this color space may be a practical method to detect LCTCs during angioscopy. Therefore, we tested in an experimental model the ability of a quantitative colorimetric system based on the L*a*b* color space to measure yellow color intensity of atherosclerotic plaques during angioscopy, and used this system to characterize the color of LCTCs.

Methods

Image acquisition system

Clinically available angioscope catheters (Vecmova, Clinical Supply Co., Gifu, Japan) were used. The imaging bundle in the catheter consists of 3,000 individual silica optical fibers and the lens allows a field of view of 70° with an imaging depth >2 mm. The rest of the system includes a xenon lamplight source (Baxter OPTX 300, Baxter Laboratories, Irvine, CA) and a charge-coupled device (CCD) camera with National Television System Committee (NTSC) color system (Baxter OPTX 5000, Baxter laboratories). When white balancing, dry white paint oil (Pure White of Designers Gouache, Winsor & Newton, London, UK) was used, and light intensity was adjusted to the maximum to enhance the white color at the periphery of the image field.

Quantitative colorimetric system

The video signal was converted from analog to digital (A/D) by a converter (ADVC-100, Canopus Co., Kobe, Japan), which was directly connected to both the S (Y/C) signal output of the CCD camera and the 6 pin IEEE1394 connector of a laptop computer (Macintosh Powerbook G4, Apple Computer, Inc. CA). The display of the laptop computer was adjusted to the color temperature = CIE D65 (based on the color temperature of xenon light) and the gamma = 2.2 (based on the definition in NTSC system) for the better visualization of image color. The custom software based on the L*a*b* color space was installed into the computer, which allows the acquisition of a single frame image (a bitmap format) while preserving the red, green and blue (RGB) values from the CCD camera independently of the color setting in the computer, and permits the user to select a point of interest (POI) or a freehanded/rectangular/circular region of interest (ROI). The conversion from RGB values into L*a*b* values was programmed according to established formulae. In the L*a*b* color space, L* describes brightness of the color (–100 to 100). A positive value of a* describes redness of the color (0 to 100), a negative a* greenness (–100 to 0). Similarly, yellowness or blueness is expressed by coordinate b*, which is positive for yellow (0 to 100) and negative for blue (–100 to 0). The L*a*b* values for each pixel and the mean values with standard deviation (SD) in the selected ROI were expressed automatically.

Materials

In-vitro imaging sample

Three circular shaped standard color calibration samples with different color intensity (SCS-OR010, CY010 and VI010, Spectralon, Labsphere, North Sutton, NH) were prepared. The samples were placed on a platform and the angioscope catheter was suspended over the samples in a movable lever.

Ex-vivo yellow plaque model

Six porcine carotid arteries were isolated and dissected from Yorkshire swine. The Animal Care and Use Committee of Tufts New England Medical Center approved all procedures. In five formalin fixed carotid arteries, yellow paint oil (Primary Yellow of Designers Gouache, WINSOR & NEWTON, London, England) was dropped at a distal end of each artery to recreate yellow plaque models. The control sample was produced by dropping yellow paint oil on a flat plastic plate.

Ex-vivo human tissue sample

The specimens of seven carotid and three femoral arteries, excised during surgical endarterectomy from 10 patients (age 72–80 years, four males and six females), were used. Written informed consent to study excised tissue was obtained from all patients before the surgical procedure. The Institutional Review Board of Tufts New England Medical Center approved the protocol. The excised specimens were washed with saline, and 5–10 mm long by 3–6 mm wide samples were obtained from each specimen. The sample was placed in a platform attached with the scale, and the angioscope catheter was suspended over the sample in a rotating lever.

Experimental design

Determination of the optimal range of L*value to measure color

In this quantitative colorimetric system, the L*a*b* values are calculated from the RGB values. However, these RGB values can be affected, to some extent, by the components of the image acquisition system. Therefore, we examined if the RGB values were within the appropriate range for this calculation. In a fully darkened room, images of the standard sample SCS-OR010 were acquired perpendicularly under varying light intensity and distance from the

angioscope lens to the sample (3–15 mm at 1 mm intervals). These two variables were selected because they can directly affect brightness and can be visually manipulated during angioscopy in vivo. L* values were measured in all images at the same POI, and the relation of these two variables with L* values was examined.

Theoretically, within the L*a*b* color space, b* values can be represented independently of L* value. However, there are functional limitations of the CCD camera, in which an image with too high or low brightness can cause either a loss of the color or a non-linear portion of the video transfer function [11], suggesting that extreme values of L* can lead to inaccurate b* values. Therefore, to establish the optimal range of brightness L* for measuring the color, 100 images of each of the three standard samples were acquired perpendicularly at 10 different levels of light intensity and at 10 different distances from the scope lens to the sample in a fully darkened room. In each sample, the same POI in all 100 images was selected at two locations, and L* and b* values were measured in all images at 200 POIs. The range of L* values, at which measured b* values were constant, was determined from this relationship to be the "optimal brightness L*". Then, to evaluate the ability to differentiate color intensity after adjusting for brightness L*, the measured b* values with optimal brightness L* from each sample were compared with each other and with the actual b* value as known by spectroradiometry under the color temperature CIE D65.

Adjustment of brightness L* for angle of imaging and POI within the field of view

A prior study reported that the perception of color could be affected by the angle of the angioscope to the plaque surface [11], indicating that if the lesion is bigger and protrudes into the artery, such lesion may have increased yellow color intensity. Another study also showed the possible effect of the POI within the field of view [9] (i.e., center of the image versus edge), because of a light diffuser at the tip of the angioscope to reduce illumination to the edge in comparison to the center. Therefore, we explored whether adjusting brightness L* can overcome the variations in the perception of color.

(a) Angle

An image of the standard sample SCS-OR010 was acquired at four different angles (90°, 60°, 45°, 30°) under fixed light intensity and distance (3 mm) from the angioscope lens to the center of the circular sample. The whole field of view (about 26,000 pixels) was selected as the ROI, and the corresponding L* and b* values were obtained for the different angles. To test the effect of adjusting brightness L* on the b* value measurement under different angles, L* and b* values were measured in circular areas (each consisting of 600–700 pixels, which is based on the commonly observed area of yellow plaques in patients) at the center of the sample, at 90°, 60°, 45°, and 30° under a fixed distance (3 mm) from the angioscope lens to the center of the circular sample. Brightness L* was adjusted by varying the light intensity and judged to be adequate when the mean value of measured L* in the ROI was within the optimal range that was established in the prior study of the relationship between brightness and color. The measured values in the image at 90° were used as controls and compared with those at the other angles.

(b) POI

An image of the standard sample SCS-OR010 was acquired perpendicularly under fixed light intensity at a distance of 3 mm from the angioscope lens to the sample, and 10 equidistant points were established from the center of the image to the edge of the field of view as illustrated in Fig. 3(a). To test the effect of adjusting brightness L* on the b* value measurement at the different POI, for each of the 10 points, an image was acquired perpendicularly at a fixed distance (3 mm), and the obtained L* value at each POI was adjusted to its optimal range by varying the light intensity. The measured b* values from the 10 POI with adjusted brightness L* were analyzed for their distribution and compared with the unadjusted values.